C = concentration of dissolved oxygen in the liquid phase, mg/L
C^* = equilibrium concentration of dissolved oxygen, mg/L
C_o = concentration of dissolved oxygen at the grid ($Y = 0$); average measurement, ~0.5 mg/L
$CSTR$ = continuous stirred tank reactor
E_y = axial dispersion coefficient, cm^2/s
$(K_La)_D$ = volumetric mass transfer coefficient for the ADM, s^{-1}
$(K_La)_{TB}$ = volumetric mass transfer coefficient for the T-ZM (bulk zone), s^{-1}
MSE = modified standard error, mg/L
PFM = plug flow model
T-ZM = two-zone model
V_g = gas superficial velocity, cm/s
V_l = liquid superficial velocity, cm/s
x = x-axis in the concentration contour diagrams, cm
y = height of the sampling points measured from the grid (y=0), cm

Greek Letters

α = $(K_La)_{TG}/V_l$, cm^{-1}
β = $(K_La)_{TB}/V_l$, cm^{-1}
ϕ = two dimensional function obtained in the contour diagrams; relates the oxygen concentration at a point in the column to its position co-ordinates.

LITERATURE CITED

Alvarez-Cuenca, M., "Oxygen Mass Transfer in Bubble Columns and Three-Phase Fluidized Beds," Ph.D. Thesis, The University of Western Ontario, London, Ontario, Canada (1979).

Alvarez-Cuenca, M., M. A. Nerenberg, M. A. Bergougnou, and C. G. J. Baker, "Mass Transfer Models for Bubble Columns and Three-Phase Fluidized Beds," *29th Canadian Chem. Eng. Conference*, Sarnia, Ontario, Canada (1979a).

Alvarez-Cuenca, M., C. G. J. Baker, M. A. Nerenberg, and M. A. Bergougnou, "Oxygen Mass Transfer in Bubble Columns Working at Large Gas and Liquid Flow Rates," *Symp. on Fundamental Research in Heat and Mass Transfer*, Annual AIChE Meeting, San Francisco, CA (1979b).

Alvarez-Cuenca, M., M. A. Bergougnou, and M. A. Nerenberg, "Oxygen Mass Transfer in Three-Phase Fluidized Beds Working at Large Flow Rates," *International Conference on Fluidization*, Henniker, New Hampshire (1980).

Alvarez-Cuenca, M., C. G. J. Baker, and M. A. Bergougnou, "Oxygen Mass Transfer in Bubble Columns," *Chem. Eng. Sci.*, **35**, 1121 (1980a).

Alvarez-Cuenca, M., M. A. Nerenberg., and M. Bergougnou, "Oxygen Transfer in Bubble Columns and Three-Phase Fluidized Beds," *VI International Fermentation Symposium*, Paper No. F7.1.12P, London, Ontario (1980b).

Chen, G. H. and R. Vallabh, "Hold-Up and Mass Transfer in Bubble Columns Containing Screen Cylinders," *Ind. Eng. Chem. Proc. Des. Devel.*, **9**, 121 (1970).

Deckwer, W-D., R. Burckhart, and G. Zoll, "Mixing and Mass Transfer in Tall Bubble Columns," *Chem. Eng. Sci.*, **29**, 2177 (1974).

Deckwer, W-D., I. Adler, and A. Zaidi, "A Comprehensive Study on CO_2—Interphase Mass Transfer in Vertical Cocurrent and Countercurrent Gas-Liquid Flow," *Can. J. of Chem. Eng.*, **56**, 43 (1978).

Deckwer, W-D., "Bubble Column Reactors—their modelling and dimensioning," *Int. Chem. Eng.*, **19** (1), 21 (1979).

Houghton, G., A. M. McLean, and P. D. Ritchie, "Absorption of Carbon Dioxide in Water Under Pressure Using a Gas-Bubble Column," *Chem. Eng. Sci.*, **7**, 26 (1957).

Hsu, K. H., L. E. Erickson, and L. T. Fan, "Pressure Drop, Gas Hold-Up, and Oxygen Transfer in Tower Systems," *Biotech. and Bioeng.*, **19**, 247 (1977).

Hsu, H. H., K. B. Wang, and L. T. Fan, "Oxygen Transfer and Absorption Efficiencies in Bubble Columns," *Water and Sewage Works* (1975).

Mashelkar, R. A., "Bubble Columns," *British Chem. Eng.*, **5** (10), 1297 (1970).

Ostergaard, K., and W. Suchozebrski, "Gas-Liquid Mass Transfer in Gas-Liquid Fluidized Beds," *Proc. 4th European Symposium Chem. Reactor Eng.*, Pergamon Press, Oxford 21 (1968).

Ostergaard, L. and P. Fosbol, "Transfer of Oxygen Across the Gas-Liquid Interface and Gas-Liquid Fluidized Beds," *Chem. Eng. J.*, **3**, 105 (1972).

Shioya, S., N. D. P. Dang, and I. Dunn, "Bubble Column Fermenter Modelling: A comparison for pressure effects," *Chem. Eng. Sci.*, **33**, 1025 (1978).

Sharma, M. M. and R. A. Mashelkar, "Absorption with Reaction in Bubble Columns," *Inst. Chem. Eng. Symp. Series*, **28**, 10 (1968).

Spiegel, R. M., *Statistics*, McGraw Hill Inc., New York (1961).

Todt, J., J. Lucke, L. Schurgel, and A. Renken, "Gas Hold-Up and Longitudinal Dispersion in Different Types of Multiphase Reactors and Their Possible Application for Microbial Processes," *Chem. Eng. Science*, **32**, 369 (1977).

Yoshida, F. and K. Akita, "Performance of Gas Bubble Columns: Volumetric Liquid-Phase Mass Transfer Coefficient and Gas Hold-Up," *AIChE J.*, **11**, 9 (1965).

Manuscript received March 3, 1980; revision received July 14, and accepted July 16, 1980.

Bacterial Population Dynamics in Batch and Continuous-Flow Microbial Reactors

Calculations of the distribution of states in cell populations grown in well-mixed, isothermal batch and continuous flow reactors are presented. By restricting the analysis to a class of bacteria for which cell division control may be modeled using overlapping timers, analytical results are obtained for many cell population characteristics in terms of the growth rate history. This required growth rate trajectory is evaluated using a separate overall reactor model. The simulation results conform qualitatively to available experimental data and suggest new experiments for further testing of the single-cell model.

Y. NISHIMURA
and
J. E. BAILEY
Department of Chemical Engineering
University of Houston
Houston, TX 77004

SCOPE

Many processes, including reactors used to grow microorganisms or to utilize their catalytic assemblies, involve dispersed phases or entities. It has long been recognized that the performance of such processes depends in general on the distribution of states over the individual particles which constitute the dispersed phase. Process mathematical modeling which includes determination of the distribution of states usually leads to population balance equations (Fredrickson et al., 1967; Ramkrishna, 1979). These models, typically of integro-partial differential equation form, are rarely amenable to analytical

Y. Nishimura is on leave from Nagoya University, Nagoya, Japan.
Correspondence concerning this paper should be addressed to his current address: Department of Chemical Engineering, California Institute of Technology, Pasadena, CA 91125.

solution, and determining approximate numerical solutions is also often a difficult task. These problems are exacerbated in the case of microbial reactor modeling. Because single living cells are themselves complex and adaptive chemical reactors, they may require a multicomponent representation, thereby substantially complicating their population balance models.

To minimize the difficulties in formulating and solving microbial population models, careful attention should be focused on the growth and regulatory features of the particular organism of interest. The bacterium *Escherichia coli* has been chosen for this study for several reasons. First, this organism has been more completely studied and is better understood than any other living thing. In particular, research on *E. coli* indicates that the single cell controls division and DNA synthesis based on timers which are started at certain critical cell mass values. These features of cellular operation provide structure for the modeling problem useful for its solution.

Models for microbial reactors containing *E. coli* populations will likely be useful for related types of bacteria. Greater large-scale utilization of these micro-organisms in the future is expected, since they are now the subjects of intensive recombinant DNA research. It is widely believed that many pharmaceuticals and other fermentation products currently manufactured using molds or mammalian cells will be produced in the future at much higher rates using bacteria modified by gene-splicing technology.

CONCLUSIONS AND SIGNIFICANCE

Many properties of a bacterial population, including mass concentration, number concentration, overall DNA concentration, the frequency functions for cell mass and cell DNA content, and cellular DNA configuration, have been determined, in most cases without recourse to population balance equations. The results are applicable in both steady-state and transient conditions. The analysis has a disadvantage in that the cellular specific growth rate $\mu(t)$ is considered to be a known function of time.

Subject to the assumptions of the single-cell model, the cellular specific growth rate is readily available for well-mixed, steady-state, continuous flow reactors. In this case, the frequency function for DNA for the cell population is very sensitive to reactor mean residence time. Also, as mean residence time increases, average cellular mass and DNA content declines, but their ratio (average cell DNA content)/(average cell mass) increases. These results are consistent with experimental observations (Maaløe, 1960).

Overall reactor transients can be approximated in many cases by a separate model which considers only nutrient and total cell mass concentrations. A standard model of this class has been used to calculate $\mu(t)$ for two different examples: a batch process and a flow-rate step change for a continuous flow reactor. The resulting growth rate transients provide the needed input to determine all of the cell population characteristics listed above.

Mean cell mass and the ratio of mean cell DNA content to mean cell mass follow the same trends during the batch as have been reported for many micro-organisms. Changes with time in cell population characteristics in both examples reflect a memory phenomenon which arises from the single-cell timer control mechanism. This results in dependence of population properties at a given time on the growth rate history during the previous hour. This memory interval is identical to the running time of the cellular control timer.

Recognition of these lags in achievement of steady-state or balanced exponential growth in the population is important for proper interpretation of experimental data and for design of process controllers. These results may also assist in developing improved models for product formation in bacterial reactors. The cell population results may be used in connection with many other overall reactor models, including those which consider spatial variations in reactor conditions. Finally, this work clearly illustrates the importance of fundamental knowledge of single cell characteristics in developing and solving models for population dynamics in microbial reactors.

To model the dynamics of *E. coli* and related bacteria, it is necessary to consider certain fundamental aspects of single cell operation. For this organism under most conditions, synthesis of cell mass and of DNA, the genetic material, appear to be interlocked with each other and with control of cell division. Synthesis of DNA is initiated whenever the cell mass attains certain critical values (Donachie, 1968), and the duration of DNA synthesis and the time from its initiation until cell division are independent of growth rate (Cooper and Helmstetter, 1968). Several authors have noted that the cell likely has no means of monitoring its mass, and several other more physically plausible mechanisms for control of initiation of DNA synthesis have been proposed (Helmstetter and Cooper, 1968; Pritchard et al., 1969; Bleecken, 1969, 1971). However, unless special experimental cultivation methods are invoked, these models are operationally identical to the one based on cell mass.

It will be helpful here to reformulate the same model in different terms so that analyses of mass and DNA synthesis and their effects in bacterial populations can be decoupled. This approach, which involves timers controlling cell division, minimizes the need for use of somewhat specialized biological concepts and terminology in the derivations and discussions. Alternative derivations, cast in more bacteriological and formal mathematical veins, of several of the succeeding results are available elsewhere (Nishimura and Bailey, 1979). A timer formalism similar to that employed below was used in the computer simulation model for bacterial population dynamics presented by Margolis and Cooper (1971).

BACTERIAL POPULATION DYNAMICS

It will be assumed that $m_{\min} = m^*$ is the minimum possible mass for a single cell, and that the cell starts a timer whenever its mass m attains one of the critical values $2^n m^*$; $n = 1, 2, 3, \ldots$ After the timer has run for a fixed time, which will be denoted L, the cell and all of its contents divide in half, giving two identical daughter cells. It is important to note that the timer span L is presumed to be independent of growth rate. Also, the timer mechanism introduced here does result in a multivariable (cell mass and timer position) single-cell model.

At any instant, a cell may have more than one active timer. Suppose, for example, that a cell containing no active timers attains mass $2m^*$ at time t_1 and reaches mass $4m^*$ by time t_2 which is in the interval $t_1 < t_2 < t_1 + L$. At time t_2, then, the first timer will have reached elapsed time $t_2 - t_1$, and a second timer

will start. At time $t_1 + L$, the cell divides, and each daughter cell inherits the second timer, which stands then at time position $t_1 + L - t_2$. When the second timer runs out at time $t_2 + L$, both daughter cells divide.

These characteristics, while apparently quite complicated, lend themselves to an analytical solution for population dynamics. The change in single cell mass with time is presumed governed by:

$$\frac{dm(t)}{dt} = \mu(t)m(t); \qquad m(t_o) = m_o \tag{1}$$

where, for the moment, $\mu(t)$ is considered as a known, nonnegative, piecewise continuous function. Analysis of single cell growth with division governed by the timer model just outlined is greatly facilitated by introducing a new mass variable w defined by:

$$w \triangleq \log_2 (m/m^*) \tag{2}$$

From Eqs. 1 and 2 it follows that:

$$w(t) = w(t_o) + \int_{t_o}^{t} k(\tau)d\tau \tag{3}$$

where

$$k(t) \triangleq \mu(t)/\ell n\ 2 \tag{4}$$

Thus, in w-coordinates, exponential growth appears as a simple linear increase, the magnitude of which is independent of the cell's initial w-value. Furthermore, the masses at which timers are started are integer values of the cell's w-coordinate. Therefore, a cell with w-value $w(t)$ at time t has $[w(t)]$ active timers: $[\cdot]$ here denotes the greatest integer function. Also in the w-coordinate, cell division implies a reduction of unity in cell w-value.

In the following, $f(w, t)$ will denote the frequency function for w for a cell population: thus, $f(w, t)dw$ is the fraction of the population with w-values between w and $w + dw$. The function $\phi(w, t)$, defined as:

$$\phi(w, t) = N(t)f(w, t) \tag{5}$$

where $N(t)$ is the number of cells per unit volume of culture at time t, will be called the number density function.

As an initial exercise in population dynamics, suppose that at time zero a population of cells with w-values in the interval $0 \le w < 1$ is placed in nutrient solution. This initial population, which is sometimes called a *resting* population because it has no active timers, has a number density function of the form:

$$\phi(w, 0) = \begin{cases} N(0)f_o(w); & 0 \le w < 1 \\ 0 & \text{otherwise} \end{cases} \tag{6}$$

Thus

$$\int_0^1 f_o(w)dw = 1 \tag{7}$$

As cells in this initial population grow, their w-values increase in parallel, Eq. 3. Suppose that the cells never divide for $t > 0$. The corresponding number density function, which will be noted by $\phi'(w, t)$ and called the tentative number density, is given at time $t_1 > 0$ by:

$$\phi'(w, t_1) = \begin{cases} N(t_o)f_o[w - \theta(t_1)]; & \theta(t_1) \le w < \theta(t_1) + 1 \\ 0 & \text{otherwise} \end{cases} \tag{8}$$

where

$$\theta(t) \triangleq \int_0^t k(\tau)d\tau \tag{9}$$

Next, the divisions experienced during the $[0, t]$ time interval are taken into account. This requires identification of the last timers to complete their cycle. These most recently completed

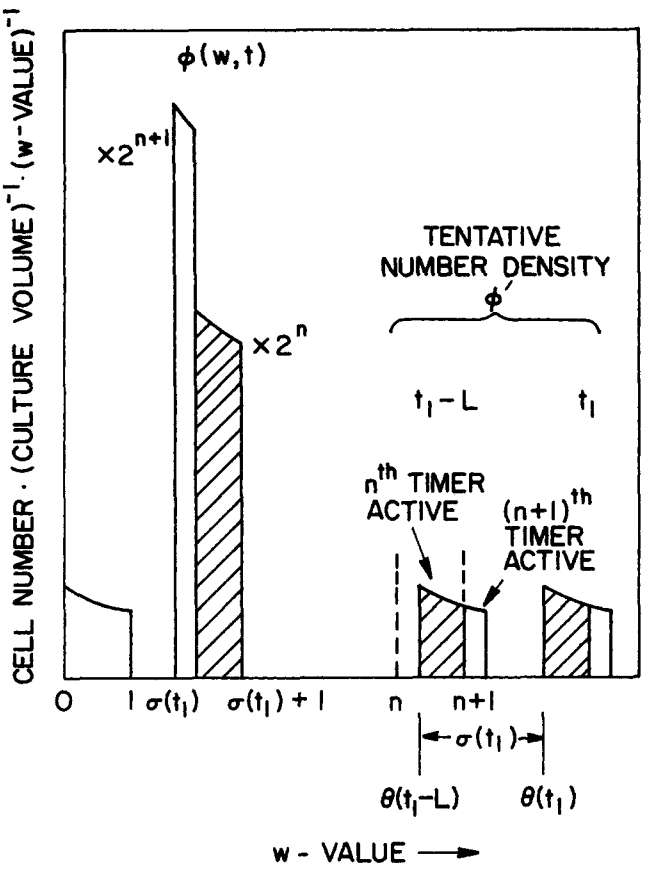

Figure 1. Schematic diagram showing the relationship among the initial number density function, the tentative number density function ϕ' at times t_1 and $t_1 - L$, and the number density function at time t_1.

timers will be the ones that were active at time $t_1 - L$; any timers started later will still be running at time t_1. Consider the tentative number density at time $t_1 - L$; in general, this function will be defined over a w-interval of length unity which will contain an integer value of the w-scale, Figure 1.

Let

$$n \triangleq [\theta(t_1 - L)] \tag{10}$$

Then, except for special cases in which $\theta(t_1 - L)$ is an integer,

$$\theta(t_1 - L) < n + 1 < \theta(t_1 - L) + 1 \tag{11}$$

Cells with w-values in the interval $[\theta(t_1 - L), n + 1)$ at time $t_1 - L$ have started their nth timer but not the $(n + 1)$st at time $t_1 - L$. By time t_1, this class of cells will have finished their nth timer (but not the $(n + 1)$st) and will be distributed over the w-interval:

$$\theta(t_1 - L) + \sigma(t_1) \le w < (n + 1) + \sigma(t_1) \tag{12}$$

where $\sigma(t)$ denotes the w-value change due to growth between times $t - L$ and t:

$$\sigma(t) \triangleq \int_{t-L}^{t} k(\tau)d\tau \tag{13}$$

Notice that, using Eqs. 9 and 13, Eq. 12 may be rewritten as:

$$\theta(t_1) \le w < \sigma(t_1) + n + 1 \tag{14}$$

Since these cells will have started and finished precisely n timers by time t_1, they will all have divided exactly n times, increasing their numbers by a factor of 2^n and decreasing their w-values by n w-units. Therefore, the actual number density function in w at time t_1 contains a nonzero component on the w-interval:

$$\theta(t_1) - n \le w < \sigma(t_1) + 1 \tag{15}$$

and defined over this w-interval as:

$$\phi(w, t_1) = 2^n N(0) f_o(w - \theta(t_1) + n) \tag{16}$$

If the same series of arguments as just constructed is applied to the part of the tentative number density defined at time $t_1 - L$ on the w-interval:

$$n + 1 \le w < \theta(t_1 - L) + 1, \tag{17}$$

it follows that these cells have divided $n + 1$ times at time t_1 and that they contribute the remaining portion of the actual number density as:

$$\phi(w, t_1) = 2^{n+1} N(0) f_o(w - \theta(t_1) + n + 1); \quad \sigma(t_1) \le w < \theta(t_1) - n \tag{18}$$

Therefore, the number density function at time t_1 is distributed entirely over the interval $[\sigma(t_1), \sigma(t_1) + 1)$, Figure 1. The function will typically contain a single discontinuity.

From $\phi(w, t)$, the number of cells per unit volume of culture may be calculated using:

$$N(t) = \int_{\sigma(t)}^{\sigma(t)+1} \phi(w, t) dw \tag{19}$$

The frequency function for w, $f(w, t)$, may be found by dividing $\phi(w, t)$ by $N(t)$, and this result may be transformed to the frequency function for mass, $f_m(m, t)$, as follows:

$$f_m(m, t) = \left[f(w, t) \frac{dw}{dm} \right]_{w=\log_2\left(\frac{m}{m^*}\right)}. \tag{20}$$

The total cell mass per unit volume of culture, $\bar{M}(t)$, may be determined from:

$$\bar{M}(t) = \int_{\sigma(t)}^{\sigma(t)+1} \phi(w, t) m^* 2^w dw \tag{21}$$

The basic unit of cellular DNA is the *genome*, which is the minimum DNA content of a living cell. One genome corresponds to one complete set of genetic information. The unit used for cellular DNA content in this work is number of genome equivalents. It has been shown that the DNA content γ of a model cell at time t is determined entirely by that cell's w-value at time t and by the growth rate history over the time interval $(t - L, t)$ (Nishimura and Bailey, 1979). This relationship may be inverted to obtain:

$$w(t) = \sigma(t) + \xi[\gamma(t), t] \tag{22}$$

where γ is the cell's DNA content. Then, the frequency function for DNA may be obtained by coordinate transformation from w to γ:

$$f_D(\gamma, t) = f[\sigma(t) + \xi(\gamma(t), t), t] \frac{d\,\xi(\gamma(t), t)}{d\gamma} \tag{23}$$

BATCH REACTOR DYNAMICS

The bacterial population at time zero will be assumed to be in a resting state. This is often the case in batch experimental studies of micro-organisms. Then, as indicated in the previous section, the initial distribution of states f_o will influence the population's behavior for all future times. This makes it important to specify f_o with some care. One reasonable approach is the following: suppose that a bacterial culture is growing at constant specific growth rate μ^*, and that growth is balanced. Here, the term "balanced" is used to indicate a growth state in which all frequency functions and the average mass and DNA content per cell are time-invariant. If this population is then transferred from nutrient solution into a solution lacking some required nutrients so that $\mu = 0$, it will decay over a time L into a resting state. The frequency function in w for this resting population will be (Nishimura and Bailey, 1979):

$$f^*(z) = (\ell n 2) 2^{1-z}; \quad 0 \le z < 1 \tag{24}$$

In the following discussion of batch reactor dynamics

$$f_o(w) = f^*(w) \tag{25}$$

will be assumed. In this case, there are no discontinuities in the number density function. Utilizing Eq. 25 in Eqs. 16 through 21, there results:

$$\phi(w, t) = \begin{cases} N(0)\ (\ell n 2) 2^{\theta(t-L)}\ 2^{(1+\sigma(t)-w)}; & \sigma(t) \le w < \sigma(t) + 1, \\ 0 & \text{otherwise} \end{cases} \tag{26}$$

$$N(t) = \begin{cases} N(0) & 0 < t < L \\ N(0) \exp\left[\int_0^{t-L} \mu(\tau) d\tau\right], & t > L \end{cases} \tag{27}$$

$$f_m(m, t) = \frac{2^{\sigma(t)+1} m^*}{m^2} \text{ for } m^* 2^{\sigma(t)} \le m < m^* 2^{\sigma(t)+1} \tag{28}$$

$$\bar{M}(t) = (2\ell n\ 2) m^* \exp\left[\int_o^t \mu(\tau) d\tau\right] \tag{29}$$

The corresponding frequency function for DNA, $f_D(\gamma, t)$, must be evaluated numerically using Eq. 23 and the $\xi \rightarrow \gamma$ mapping mentioned above.

As previously explained, it is necessary to interface these population dynamics results with a separate model of overall dynamics in the batch reactor. This model is formulated here based on Monod kinetics (Monod, 1949) and the assumption that the yield Y of cell mass produced per unit mass of limiting nutrient consumed is constant. Then, the well-mixed, isothermal batch reactor may be described in overall terms by:

$$\frac{d\bar{M}(t)}{dt} = \mu(t)\bar{M}(t), \tag{30}$$

$$\frac{dS(t)}{dt} = -\frac{1}{Y} \mu(t)\bar{M}(t), \tag{31}$$

$$\bar{M}(0) = \bar{M}_o, \qquad S(0) = S_o \tag{32}$$

with

$$\mu(t) = \frac{\mu_{\max} S(t)}{K_s + S(t)} \tag{33}$$

The symbol $S(t)$ denotes the concentration (mass per unit volume) of growth-limiting nutrient in the reaction mixture.

The parameters required to specify the system are reduced by transforming to the following dimensionless variables and parameters.

$$x(t) = \bar{M}(t)/YS_o, \qquad y(t) = S(t)/S_o$$
$$K = K_s/S_o, \qquad x_o = \bar{M}_o/YS_o \tag{34}$$

giving

$$\frac{dx(t)}{dt} = \mu(t)x(t) = -\frac{dy(t)}{dt} \tag{35}$$

with

$$x(0) = x_o, \qquad y(0) = 1, \tag{36}$$

and

$$\mu(t) = \frac{\mu_{\max} y(t)}{K + y(t)} \tag{37}$$

Eqs. 35 and 36 may be integrated, giving $y(t)$ implicitly through the formula (Bailey and Ollis, 1977):

$$(1 + x_o + K)\ell n\left[\frac{1 + x_o + y(t)}{x_o}\right]$$

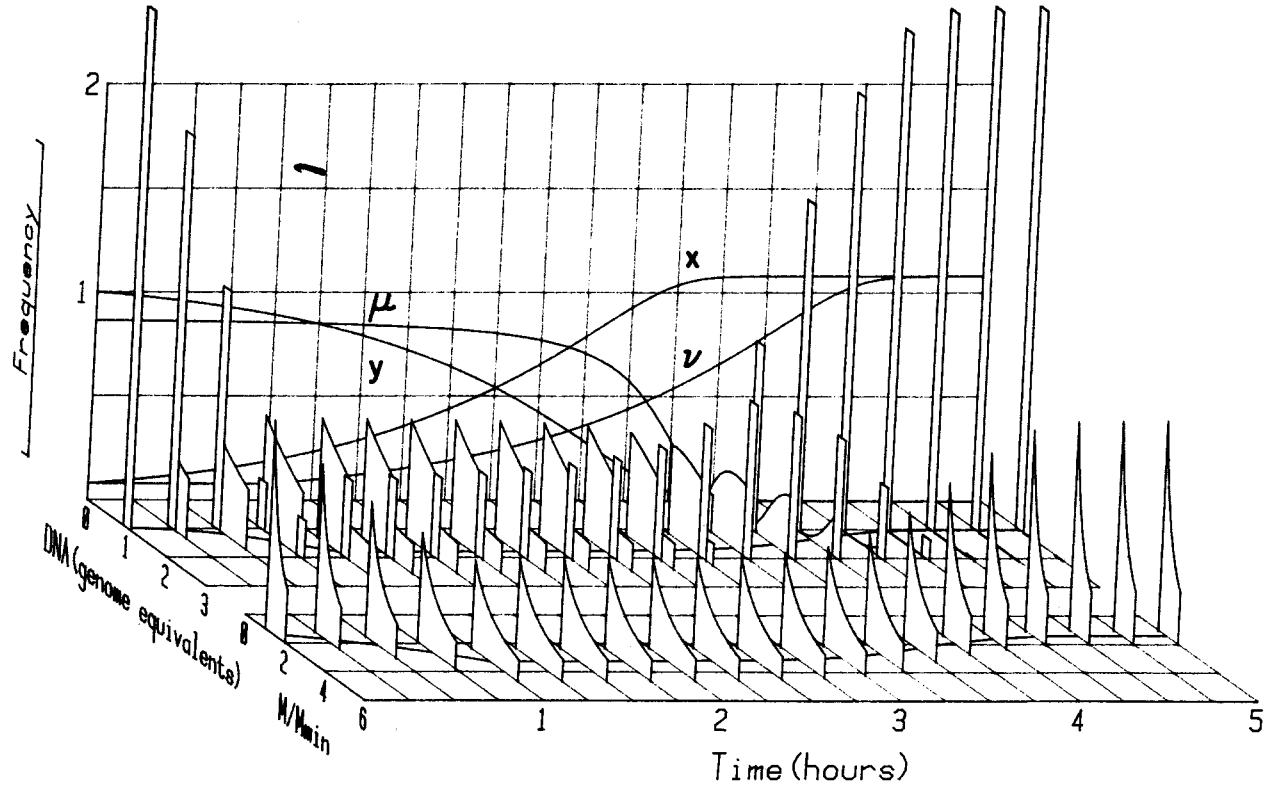

Figure 2. Batch reactor simulation results. The curves marked μ, y, x, and ν are specific growth rate and dimensionless substrate, cell mass, and cell number concentrations, respectively. The ordinate scale for these quantities is linear and ranges from zero to two as shown. Sequences of curves in rear and front sections of the figure are frequency functions for DNA and mass, respectively.

$$- K \ell n\, y(t) = (1 + x_o)\mu_{\max}\, t \quad (38)$$

Once $y(t)$ is determined, $\mu(t)$ follows from Eq. 37. The resulting $\mu(t)$ may then be used to calculate population dynamics.

Figure 2 illustrates the results of such calculations for the parameter values $\mu_m = 0.95\ h^{-1}$, $x_o = 0.08$, and $K = 0.1$. The curves on the rear vertical panel are the specific growth rate μ, the dimensionless nutrient and cell mass concentration y and x, and a dimensionless cell number concentration $\nu = (\bar{M}(0)N(t))/(YS_oN(0))$, respectively. The rear sequence of functions are the frequency functions for DNA at the indicated times during the batch. The narrow, blocked vertical bars appearing in some of these are symbolic representations of impulse functions which arise at integer genome values. The height of these bars is scaled to correspond to the corresponding inpulse magnitude. The front sequence of curves are the frequency functions for cell mass. The heavy lines sometimes visible in the front and rear floor panels are the mean cell mass and mean cell DNA content, respectively. A different view of the frequency functions which more clearly shows their changes during the batch is provided in Figure 3.

Many of the trends evident in this simulation are consistent with experimental observations of batch microbial reactors (Herbert, 1961). The lag of cell number increase relative to total cell mass increase, giving a larger average mass for cells during active growth of the culture, is one such feature. Another is the decline in the ratio of average DNA per cell to average cell mass during the early period of the batch. Reversal of these trends as the growth rate approaches zero also agrees with experiment. This simulation does not exhibit the lag in initiation of culture growth which is often observed to occur just after inoculation of a microbial batch reactor. The overall dynamic model of this system could, however, be modified to provide this result.

One interesting result is the transient in reaching the resting state after the growth rate has become approximately zero. During this transient, the frequency function for DNA is sharply bimodal; the impulse at $\gamma = 2$ gradually fades and contributes to the accumulating resting-state impulse at $\gamma = 1$. Changes with time in $f_m(m, t)$ are relatively smooth, consisting of shifting and stretching according to Eq. 28. As Eq. 27 indicates, if the growth rate is nonzero until time $\hat{t}$, cell numbers will continue to increase until time $\hat{t} + L$.

STEADY-STATE AND TRANSIENT BEHAVIOR OF MICROBIAL CSTRs

To a well-mixed isothermal reactor containing a microbial culture of volume V, a sterile solution of nutrient at concentration S_o is continuously fed at flow rate $F(t)$, and culture is pumped out of the reactor at the same flow rate. Under these conditions, the total cell mass and substrate concentrations satisfy:

$$\frac{d\bar{M}(t)}{dt} = [\mu(t) - D(t)]\bar{M}(t) \quad (39)$$

and

$$\frac{dS(t)}{dt} = D(t)[S_o - S(t)] - \frac{1}{Y}\mu(t)\bar{M}(t) \quad (40)$$

respectively, where the dilution rate $D(t)$, equal to the number of reaction mixture volumes fed through the reactor per unit time, is defined by:

$$D(t) = F(t)/V \quad (41)$$

For steady-state reactor operation at time-invariant dilution rate D^*, it follows from $d\bar{M}(t)/dt = 0$ and Eq. 39 that either $\bar{M}^*$ is zero, a pathological situation in which the microbial culture has been washed out of the reactor, or the specific growth rate μ^* must be equal to D^*. For transient reactor operation, calculations similar to those for the batch reactor are necessary to determine $\mu(t)$. In the computations presented below, the specific growth rate has been assumed to depend on nutrient concentration according to Eq. 33.

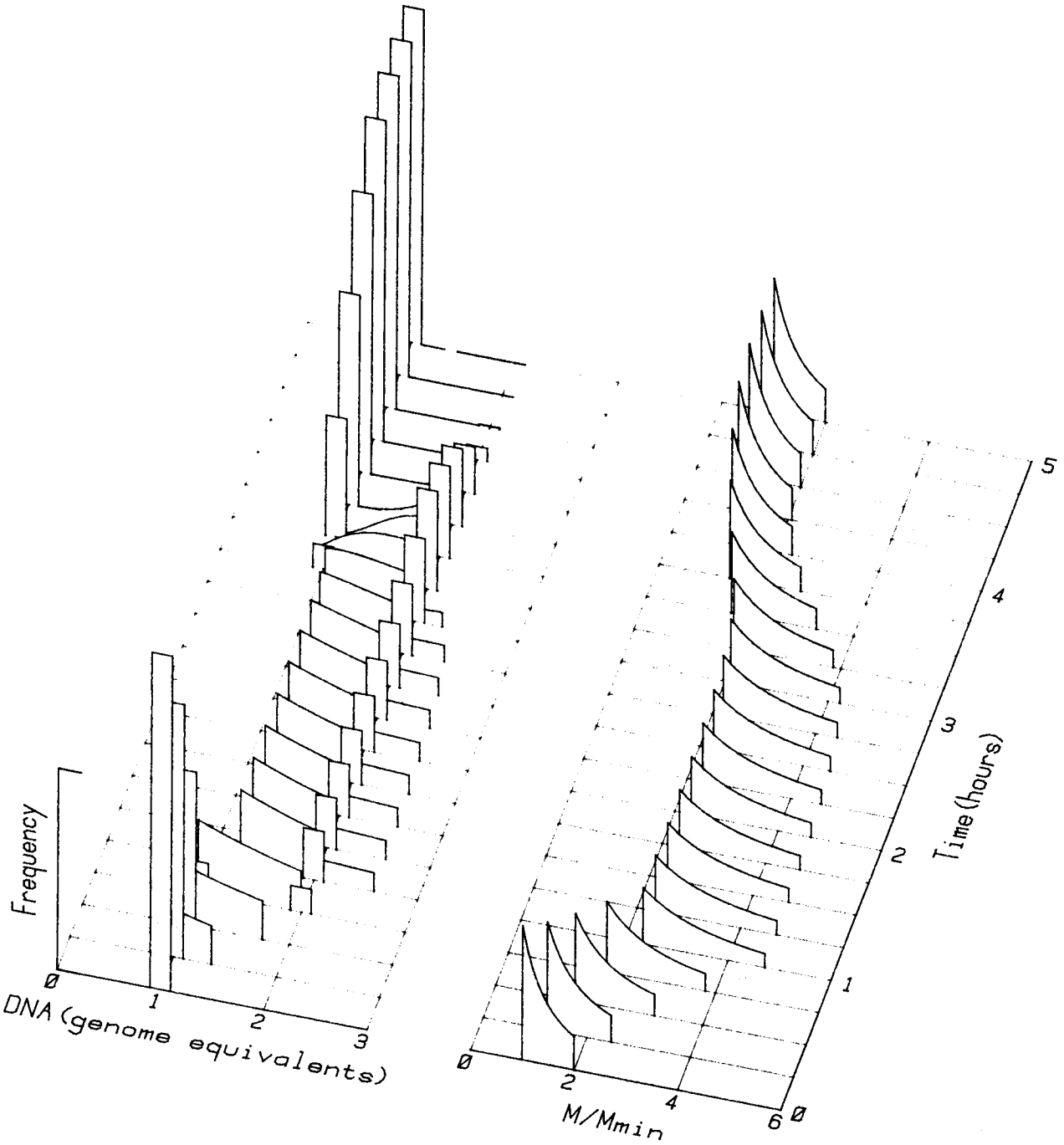

Figure 3. Another view of the sequence of DNA and mass frequency functions at different times during batch growth of bacteria.

A description of bacterial population dynamics in the CSTR may be readily obtained from the results above. This is most easily demonstrated by establishing a simple relationship between the number density function for w in a closed system and this function for a CSTR with the same growth rate trajectory $\mu(t)$. The population balance equation for the closed system is (Fredrickson, et al., 1967; Ramkrishna, 1979):

$$\frac{\partial \phi(w, t)}{\partial t} = - k(t) \frac{\partial \phi(w, t)}{\partial w} \tag{42}$$

and the corresponding equation for the population in a CSTR is:

$$\frac{\partial \phi(w, t)}{\partial t} = - k(t) \frac{\partial \phi(w, t)}{\partial w} - D(t)\phi(w, t) \tag{43}$$

Suppose that the appropriate boundary conditions and identical initial conditions are applied in each case. Then, it can be shown by direct substitution that if $\phi_c(w, t)$ is a solution to the problem associated with Eq. 42, $\phi_f(w, t)$ given by

$$\phi_f(w, t) = \phi_c(w, t) \exp \left[- \int_0^t D(\tau) d\tau \right] \tag{44}$$

satisfies the corresponding problem for the CSTR including Eq. 43.

Clearly the influence of the continuous flow through the vessel is to influence the magnitude of $\phi_f(w, t)$ but not its shape; i.e., not the dependence on w at a given t. Recalling Eq. 5, this means that $N(t)$ is modified in the CSTR, but the frequency function $f(w, t)$ is not. This implies that the frequency functions for w, m, and γ derived earlier for a closed system apply to the

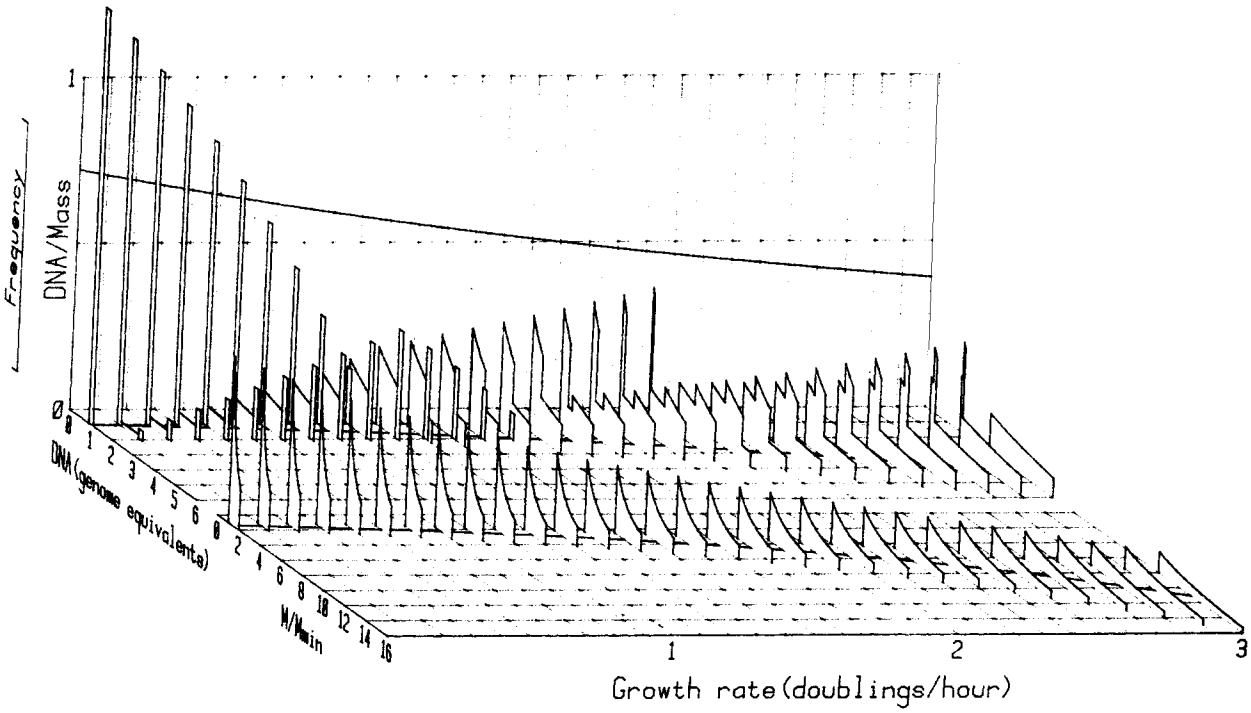

Figure 4. Properties of bacterial populations in steady-state CSTRs at different dilution rates. Rear panel illustrates the ratio of mean dimensionless cell mass to mean cell DNA content. Frequency functions displayed as in Figure 2.

CSTR. In particular, if the population used to start up the CSTR has a frequency for w of the form of Eq. 24, Eq. 28 is valid for the continuous-flow reactor. The corresponding $f_D(\gamma, t)$ function must be calculated from Eq. 23 as in the batch case.

In the case of steady state operation with $\mu^* = D^*$, the function $\sigma(t)$ assumes the constant value:

$$\sigma^* = LD^*/\ell n\ 2 \tag{45}$$

The DNA content and cell mass frequency functions for various growth rates, plotted vs. doublings per hour $= D^*/\ell n\ 2$, are illustrated in Figure 4. As in Figure 2, the average masses and DNA contents per cell are drawn on the base panels. The ratio of these average values, which is shown on the back panel, follows the declining trend observed experimentally (Schaechter et al., 1958).

As a final example, the response of the microbial CSTR to a step change in flow rate will be investigated. It will be assumed that at time zero the CSTR is in the steady state corresponding to $D_1 = 0.8\ h^{-1}$. This CSTR was started up earlier using a resting state population with $f_0(w)$ given by Eq. 25. Then, for times larger than zero, the flow rate is increased giving $D_2 = 1.6\ h^{-1}$ for $t > 0$. The other parameter values used in this simulation are:

$$\mu_m = 2.0\ h^{-1}, \qquad K = 0.1 \tag{46}$$

The transient responses $\bar{M}(t)$, $S(t)$, and $\mu(t)$ are calculated employing Eqs. 33, 38, and 39. With $\mu(t)$ known, $\sigma(t)$ and hence $f_m(m, t)$ and $f_D(\gamma, t)$ may be evaluated.

A slight modification of Eq. 27 is necessary for correct determination of $N(t)$. This change is required because it was assumed in deriving Eq. 28 that $\mu(t)$ was zero for negative t. Such is not the case for this CSTR step experiment. The rationale for the revised formula can be understood by referring to the batch reactor results above; its derivation is available elsewhere (Nishimura and Bailey, 1979). It was noted in the batch reactor simulations that cell number concentration displays a memory effect: after batch growth stopped, cell numbers continued to increase for the next L time units. This means that $N(t)$ in the CSTR shift experiment will retain some effects from the preshift steady state during the time interval $0 < t < L$. The necessary formula for this case is:

$$N(t) = N(0) \exp\left[\int_{-L}^{t-L} \mu(\tau)d\tau\right] \exp\left[-\int_{0}^{t} D(\tau)d\tau\right] \tag{47}$$

All of the simulation results are collected in Figure 5. The dimensionless cell number concentration in this plot is $N(t)x_1/(N(0) \exp(D_1L))$ where x_1 is the dimensionless total cell mass concentration at the steady state corresponding to dilution rate D_1. Here, the change in specific growth rate $\mu(t)$ is sufficiently slow that the lag in $N(t)$ relative to $\mu(t)$ and $\bar{M}(t)$ is not obvious. All of the transients are very smooth except for the DNA frequency functions, where again very dramatic changes occur.

DISCUSSION

The population dynamics model employed here successfully simulates some of the characteristics of reactors for cultivation of *E. coli* and related bacteria. However, little experimental information is available on the distribution of states in the bacterial population. Thus, this important part of the theory must await new experiments for its evaluation. It may be possible to measure approximately the $f_D(\gamma, t)$ frequency function using flow microfluorometry techniques (for example, Bailey et al., 1978). Research along these lines is currently in progress in the author's laboratory and should aid in evaluating the single-cell model considered here.

The above results for bacterial population dynamics may be used with reactor models and overall kinetics different from those employed in the previous illustrations. It is known, for example, that lags sometimes exist in growth rate responses to nutrient concentration changes, and that these effects are not simulated well using Monod kinetics. An overview of alternative approaches to reactor dynamics modeling is provided in Bailey and Ollis (1977).

The present theory of single-cell and population dynamics rests heavily on a critical assumption, the limitations of which should be recognized. The growth rate function $\mu(t)$ is presumed to be known. To calculate $\mu(t)$ from an overall reactor model independent of consideration of population details, it must be assumed that the overall culture growth rate and the

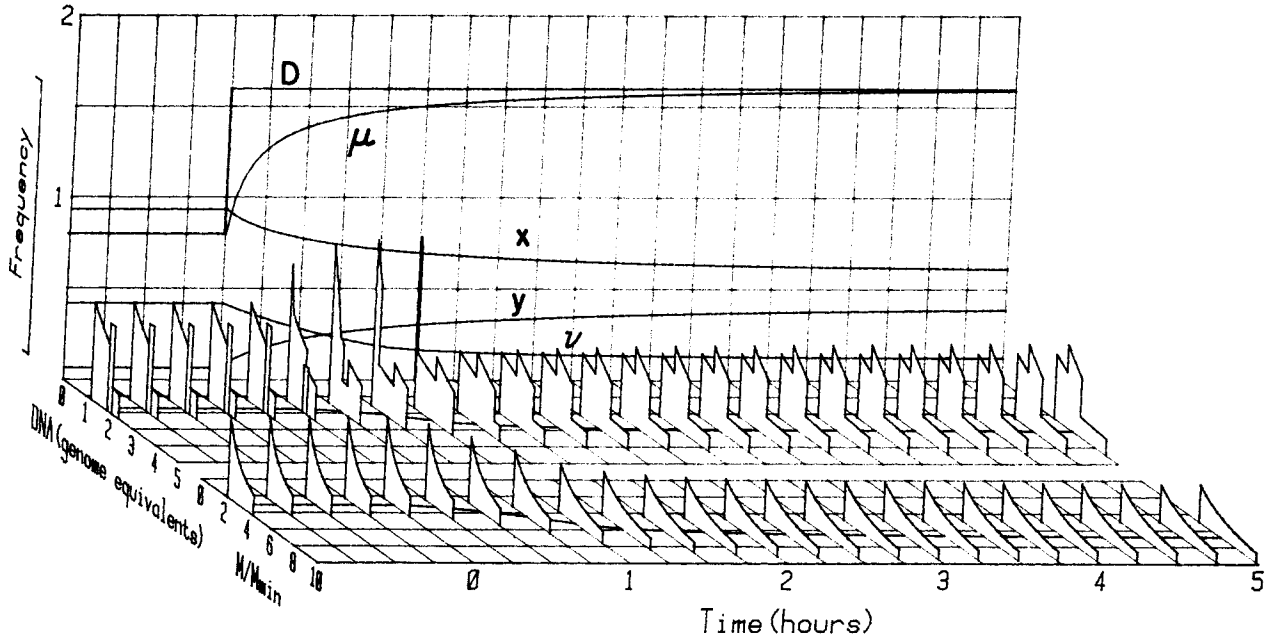

Figure 5. Calculated response of a bacterial CSTR to a step change in feed flow rate. Curves D, μ, x, y, and ν are dilution rate, specific growth rate, and dimensionless cell mass, substrate, and cell number concentrations, respectively.

rate of nutrient consumption are independent of the distribution of states in the population. This may not always be valid, and an extended theory or simulation strategy is then required. The recent modeling work by Shuler et al. (1979) should be useful in this connection.

In its present form, however, the theory can be used to construct product formation models in which the production rate of a desired microbial product by an individual cell depends on nutrient concentration, cell mass, and cell DNA content. This is expected, for example, for certain enzymes which are produced in direct proportion to the number of DNA segments in the cell which code for those enzymes (for example, Donachie and Masters, 1969). Letting $r_p(w, S, t)$ denote the rate of product formation at time t for a cell characterized by its w-value in a solution of nutrient at concentration S, the rate of product formation per unit volume of culture $\bar{r}_p$ is given by:

$$\bar{r}_p(S, t) = \int_{\sigma(t)}^{\sigma(t)+1} \phi(w, t) r_p(w, S, t) dw \qquad (48)$$

ACKNOWLEDGMENTS

The authors are indebted to the University of Houston and to the National Science Foundation for financial support of this research.

NOTATION

D = F/V, dilution rate
f = frequency function
f^* = frequency function given in Eq. 24
F = volumetric flow rate
k = growth rate function defined in Eq. 4
K = dimensionless kinetic parameter
K_s = growth rate saturation parameter
L = time duration of cell division timer
m, M = cell mass
m^* = minimum cell mass = M_{min}
$\bar{M}$ = total mass of cells per unit volume of culture
n = an integer
N = number of cells per unit volume of culture
r_p = single cell product formation rate
$\bar{r}_p$ = overall product formation rate
S = mass of growth-limiting nutrient per unit volume of culture
t = time
V = reaction mixture volume
x = dimensionless cell mass concentration
y = dimensionless limiting nutrient concentration
Y = yield factor; mass of cells formed per mass of limiting nutrient consumed

Greek Letters

γ = DNA content in genome equivalents
θ = function defined in Eq. 9
μ = specific growth rate
μ_{max} = maximum specific growth rate parameter
ξ = $w - \sigma$
σ = function defined in Eq. 13
ϕ = number density function
ϕ' = tentative number density function

Subscripts

c = closed
C = DNA
f = flow
m = mass
o = initial

LITERATURE CITED

Bailey, J. E., J. Fazel-Madjlessi, D. N. McQuitty, L. Y. Lee, and J. A. Oro, "Measurement of Structured Microbial Population Dynamics by Flow Microfluorometry," *AIChE J.*, **24**, 570 (1978).

———, and D. F. Ollis, *Biochemical Engineering Fundamentals*, McGraw-Hill, New York (1977).

Bleecken, S., "Duplication of the Bacterial Cell and Its Initiation," *J. Theoret. Biol.*, **24**, 137 (1969).

Bleecken, S., " "Replisome"—Controlled Initiation of DNA Replication," *J. Theoret. Biol.*, **32**, 81 (1971).

Cooper, S., and C. E. Helmstetter, "Chomosome Replication and the Division Cycle of *Escherichia coli* B/r," *J. Molecular Biol.*, **31**, 519 (1968).
Donachie, W. D., "Relationships Between Cell Size and Time of Initiation of DNA Replication," *Nature*, **219**, 1077 (1968).
Donachie, W. D., and M. Masters, "Temporal Control of Gene Expression in Bacteria," *The Cell Cycle*, G. L. Whitson and I. L. Cameron, eds., Academic Press, New York (1969).
Fredrickson, A. G., D. Ramkrishna, and H. M. Tsuchiya, "Statistics and Dynamics of Procaryotic Cell Populations," *Math. Biosci.*, **1**, 327 (1967).
Helmstetter, C. E., and S. Cooper, "DNA Synthesis During the Division Cycle of Rapidly Growing *Escherichia coli* B/r," *J. Molecular Biol.*, **31**, 507 (1968).
Herbert, D., "The Chemical Composition of Micro-Organisms as a Function of Their Environment," *Symp. Soc. Gen. Microbiol.*, **11**, 391 (1961).
Maaløe, O., "The Nucleic Acids and the Control of Bacterial Growth," *Symp. Soc. Gen. Microbiol.*, **10**, 272 (1960).
Margolis, S. G., and S. Cooper, "Simulation of Bacterial Growth, Cell Division, and DNA Synthesis," *Comput. Biomed. Res.*, **4**, 427 (1971).
Monod, J., "The Growth of Bacterial Cultures," *Ann. Rev. Microbiol.*, **3**, 371 (1949).
Nishimura, Y., and J. E. Bailey, "On the Dynamics of Cooper-Helmstetter-Donachie Procaryote Populations," *Math. Biosci.*, **51**, 305 (1980).
Prichard, R. H., P. T. Barth, and J. Collins, "Control of DNA Synthesis in Bacteria," *Symp. Soc. Gen. Microbiol.*, **19**, 263 (1969).
Ramkrishna, D., "Statistical Models of Cell Populations," *Advance in Biochemical Engineering 11*, T. K. Ghose, A. Fiechter, and N. Blakebrough, eds., Springer-Verlag, Berlin (1979).
Schaechter, M., O. Maaløe, and N. O. Kjeldgaard, "Dependency on Medium and Temperature of Cell Size and Chemical Composition During Balanced Growth of *Salmonella typhimurium*," *J. Gen. Microbiol.*, **19**, 592 (1958).
Shuler, M. L., S. Leung, and C. C. Dick, "A Mathematical Model for the Growth of A Single Bacterial Cell," *Annals N.Y. Acad. Sci.*, **326**, 35 (1979).

Manuscript received January 14, 1980; revision received May 2, and accepted May 12, 1980.

Effective Diffusivity by The Gas Chromatography Technique: Analysis and Application to Measurements of Diffusion of Various Hydrocarbons in Zeolite NaY

The gas chromatography technique was applied to measurements of diffusion of n-butane in zeolite NaY. The linear chromatography theory failed to explain these results quantitatively, and a significant system nonlinearity was demonstrated. This nonlinearity is likely associated with non-Fickian diffusion. Order of magnitude estimates of the diffusivity could still be obtained, however. Over the range of temperatures 105 to 240°C, the n-butane diffusivities were in the range 10^{-8} to 10^{-6} cm^2/s. Similar results were obtained with n-hexane and calculated diffusivities were about an order of magnitude smaller than the corresponding n-butane values. In contrast, limited experiments with cyclohexane, 2, 2-dimethylbutane, and *trans*-decalin were entirely consistent with the linear chromatography theory. At the measurement temperatures, the intracrystalline diffusion was too rapid to be detected in any of these systems. Attempts to operate at lower temperatures where diffusion might be significant were frustrated by extensive peak broadening and concomitant loss of detector response.

L.-K. P. HSU
and
H. W. HAYNES, JR.
Chemical Engineering Department
University of Mississippi
University, MS 38677

SCOPE

Large pore zeolites and in particular the faujasite-type zeolites (zeolites *X* and *Y*) have seen widespread applications as cracking and isomerization catalysts (Haynes, 1978). In spite of this, information concerning mass transfer in the large pore zeolites is only fragmentary. When studying the information that is available, one frequently observes discrepancies of several orders of magnitude in the diffusivities reported by different investigators employing different techniques of measurement. Many times these discrepancies arise from failure of the system equations to properly describe all important physical phenomena. This can go unrecognized if no attempt is made to compare the model predictions with the experiment.

One of the more popular methods for evaluating effective diffusivities in heterogeneous catalysts is based on gas chromatography. In earlier work from our laboratory, the GC-technique was successfully employed to evaluate diffusivities in small pore zeolites (Sarma and Haynes, 1974a) and these results were confirmed by independent investigators using an adsorption rate technique (Shah and Ruthven, 1977).

One objective of the present investigation was to apply the GC-technique to measurements of diffusion of various hydrocarbons in large pore zeolites. A necessary prerequisite was to provide a rigorous test of the linear chromatography theory in its ability to describe the experimental results.

Several important improvements were incorporated into the data analysis procedure to provide the most meaningful com-

Correspondence concerning this paper should be addressed to H. W. Haynes, Jr.

0001-1541-81-4216-0081-$2.00.